Article

The Birefringence and Extinction Coefficient of Ferroelectric Liquid Crystals in the Terahertz Range

Ying Ma [1,*], Yuhang Shan [1], Yongning Cheng [1], Ruisheng Yang [2], Hoi-Sing Kwok [3] and Jianlin Zhao [1]

1   Key Laboratory of Light Field Manipulation and Information Acquisition, Ministry of Industry and Information Technology, School of Physics Science and Technology, Northwestern Polytechnical University, Xi'an 710129, China; 2021264937@mail.nwpu.edu.cn (Y.S.); yncheng@mail.nwpu.edu.cn (Y.C.); jlzhao@nwpu.edu.cn (J.Z.)
2   MOE Key Laboratory of Material Physics and Chemistry under Extraordinary Conditions, School of Physical Science and Technology, Northwestern Polytechnical University, Xi'an 710129, China; rsyang@mail.nwpu.edu.cn
3   State Key Laboratory (SKL) on Advanced Displays and Optoelectronics Technologies, Department of Electronic and Computer Engineering, Hong Kong University of Science and Technology, Kowloon 999077, Hong Kong; eekwok@ust.hk
*   Correspondence: maying916@nwpu.edu.cn

Abstract: In this paper, the refractive index and extinction coefficient of ferroelectric liquid crystals have been examined by the terahertz time-domain spectroscopy system. Two modes of ferroelectric liquid crystal materials, deformed helix ferroelectric liquid crystal (DHFLC), and electric suppressed helix ferroelectric liquid crystal (ESHFLC) are tested as experimental samples. Nematic liquid crystal (NLC) was also investigated for comparison. The birefringence of DHFLC 587 slowly increases with the growth of frequency, and it averages at 0.115. Its extinction coefficients gradually incline to their stable states at 0.06 for o-wave and 0.04 for e-wave. The birefringence of ESHFLC FD4004N remains between around 0.165 and 0.175, and both of its e-wave and o-wave extinction coefficients are under 0.1, ranging from 0.05 to 0.09. These results of FLC will facilitate the examination and improve the response performance of THz devices using fast liquid crystal materials.

Keywords: liquid crystal; birefringence; extinction; terahertz

1. Introduction

Terahertz (THz) radiation refers to a radiation wave with a frequency of 0.1 to 10 THz and wavelength of 30 μm to 3000 μm. Due to its unique spectrum range, it includes both properties of microwave radiation and infrared radiation, such as great penetration to non-conducting surfaces and traveling in line-of-sight without ionizing [1]. Nowadays, THz radiation has been implemented in a great number of researches and applications such as imaging [2–4], sensing [5–8], fast or wireless communication systems [9–13], and medical diagnoses for diseases [14–17]. Also, the THz wave has been widely used in photonic and electronic devices [18–21] and modulation systems [22–24].

Liquid crystal (LC) is a substance composed of rod-like molecules with particular directions [25], and these molecules can modulate and regulate optical field [26,27], especially in the THz domain due to its high birefringence in the THz region [28]. Thus, LC is a suitable material for tunable photonic devices working in the THz environment, such as a voltage-controlled THz phase shifter and quarter-wave plate [29–33]. Recently, plasmon-induced LC metamaterial was implemented to fabricate an electrically tunable THz modulator with a large modulation depth and low insertion loss [34]. Therefore, it is of great importance to measure the birefringence of LC material in THz devices in order to test and improve their performance [35,36].

Currently, to enhance the response speed, many new kinds of LC have been applied in scientific research and industrial productions. For example, blue-phase LC [37,38]

and cholesteric LC [39,40] were used in tunable optical devices to achieve a fast switch. However, they suffer from problems of controlling with a high voltage and difficult material processing procedures and conditions. Recently, ferroelectric LC (FLC) materials have proven their excellent optical quality and fast response time to the microsecond level [41,42], making them promising materials for THz devices. In addition, the birefringence properties of NLC [43] and blue-phase LC [44] in the THz region have been researched, but the properties of FLCs have rarely been investigated.

In this paper, the refractive index and extinction coefficient of FLC in the THz range were measured by a THz time-domain spectroscopy system. Two FLC modes, including deformed helix FLC (DHFLC) and electric suppressed helix FLC (ESHFLC), were tested in this system. NLC as the compared sample was also investigated. After Fourier transformation and several calculations for the THz wave amplitudes in a time-domain, the birefringence and extinction coefficient of each LC material in the THz range are acquired. The birefringence of DHFLC 587 averages 0.115 between frequency from 0.2 THz to 1 THz. Its extinction coefficients remain at 0.06 for o-wave and 0.04 for e-wave. Meanwhile, the birefringence of ESHFLC FD4004N is around 0.165 to 0.175 in the same THz frequency-domain, and its e-wave extinction coefficient is about 0.01 smaller than its o-wave extinction coefficient, which ranges from 0.05 to 0.09. These results of FLC will facilitate the examination of and improvement in the performance of THz devices using FLC materials.

2. Experiment

To align the LC molecules used in the following experiments, a polarization photosensitive alignment sulphonic azo-dye (SD1) is chosen as the aligning material for its high anchoring energy, lack of mechanical damages, and minimized unwanted electronic charges. Under exposure from a polarized light source in the UV-to-blue spectrum, the SD1 molecule tends to orient perpendicularly to the polarization of the incident light, giving planer alignment for LC molecules. Two optically flat indium tin-oxide-coated glass plates coated with SD1 were used for preparing a sandwich-type sample holder with a cell thickness of 150 μm. After being exposed under a polarized UV light, LCs were then filled into the cells. In this work, DHFLC 587 (from P. N. Lebedev Physical Institute of Russian Academy of Sciences) was selected as the material for its high transmission in the visible spectrum and fast switching. DHFLC 587 is composed with two achiral biphenylpirimidines to form the smectic C matrix, and a chiral nonmesogenic substance with a very high twisting power [45]. The phase transitions sequence of this LC during heating up from the solid crystalline phase is Cr $\rightarrow$ 12 °C $\rightarrow$ SmC* $\rightarrow$ 110 °C $\rightarrow$ SmA* $\rightarrow$ 127 °C $\rightarrow$ Is, while cooling from smectic C* phase crystallization occurs around -10 °C–15 °C. The spontaneous polarization P_s and the tilt angle θ at room temperature are 150 nC/cm^2 and 36.5°, respectively. A ESHFLC FD4004N (DIC, Japan) was chosen for these FLC switches with a phase transition scheme as SmC*$\rightarrow$SmA$\rightarrow$N*$\rightarrow$Iso at temperatures of 72 °C, 85 °C, and 105 °C, respectively. At room temperature, the helix pitch is $P_0 = 350$ nm, spontaneous polarization $P_s = 61$ nC/cm^2, and tilt angle $\theta \approx 22.5°$. NLC E7 was used as the compared LC material, and an empty cell without LC filled was also prepared serving for comparison. Figure 1 shows the image of E7, DHFLC587, and FD4004N mixtures pictured by a polarizing optical microscope, respectively. The microscopic photos indicate a good alignment quality in this large thickness. DHFLC 587 and FD4004N were selected for their fast-switching time, with DHFLC587 having a switching time of $\tau_{on} = 175$ μs at 1.5 V/μm and $\tau_{off} = 150$ μs at 1.5 V/μm, and FD4004N having a switching time of $\tau_{0n+off} = 160$ μs at 1 V/μm.

The THz time-domain spectroscopy system shown in Figure 2 was exerted to measure the amplitude and phase of the samples during transmission in the time-domain. A femtosecond laser beam was split into two beams by the beam splitter, one as the probe beam was injected into the detector to detect the THz signal and the other one as the signal beam ran through the delay line and the THz emitter to generate the THz signal. The generated signal was transmitted through the sample and finally injected into the detector

at the same time as the probe signal. The alignment direction of the LC molecules was parallel to the polarization of the signal beam, as shown in Figure 3a. Amplitude and phase were able to be obtained from the connected computer system. Then, the sample was rotated 90° to make the alignment of the sample perpendicular to the polarization of the signal beam, as shown in Figure 3b, and the same experiment procedures were exerted. Thus, LC molecules were photoaligned in the y-axis for NLC E7 and helixes were aligned in the y-axis for FLCs, parallel to the substrates. These two time-domain results were calculated and then processed by Fourier transform to acquire the information of the refractive index and extinction coefficient. The former and latter experiment results show the refractive index and extinction coefficient of e-wave and o-wave, respectively. Therefore, the birefringence of these three different kinds of LC can be obtained from the difference in the o-wave and e-wave refractive index.
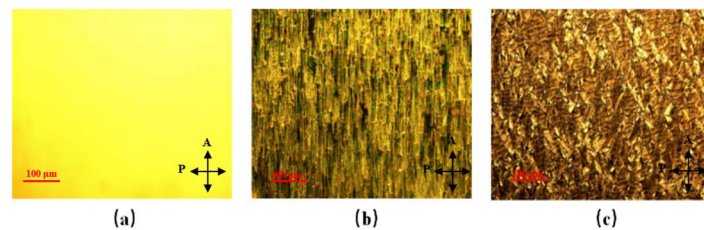
Figure 1. Microscopic pictures of E7 (**a**), DHFLC 587 (**b**), and ESHFLC FD4004N (**c**) with crossed polarizers (P and A inserted in (**a**)).
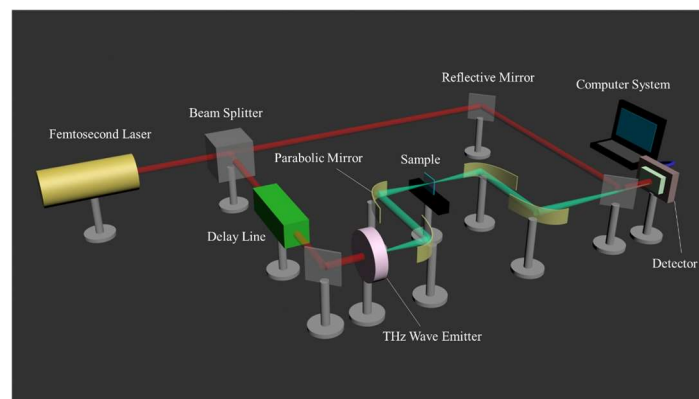
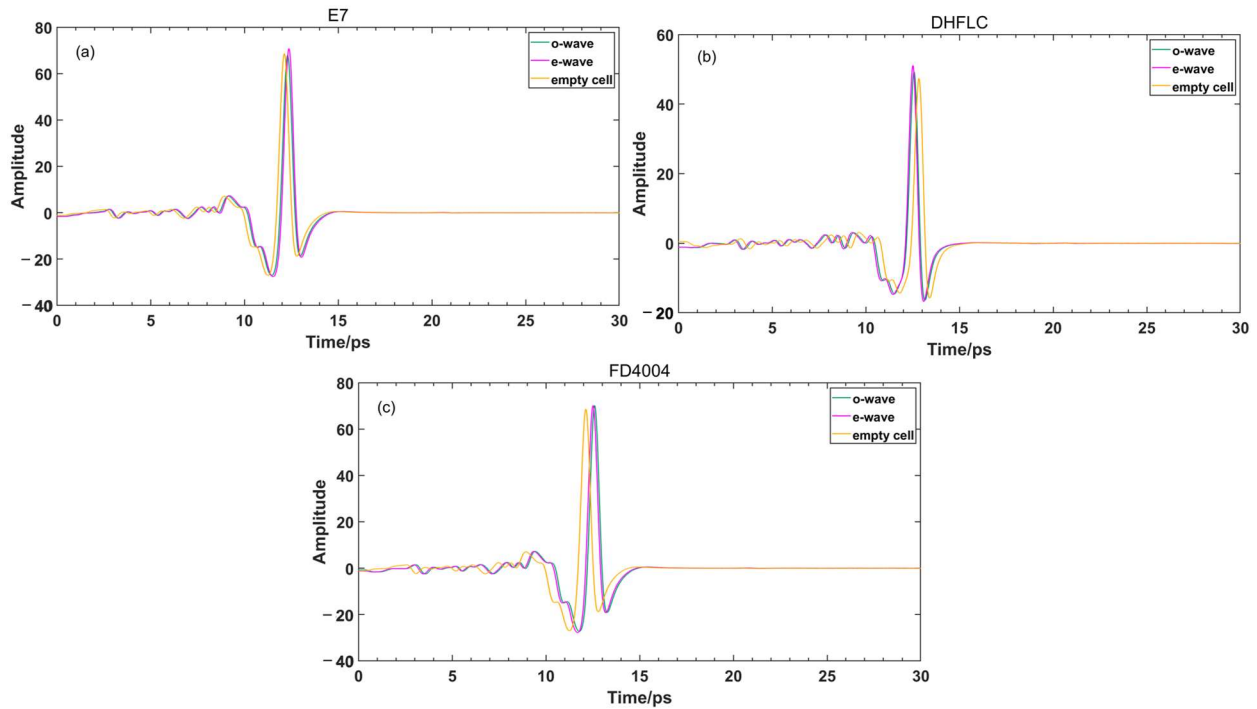**Figure 2.** Illustration of THz time-domain spectroscopy system.
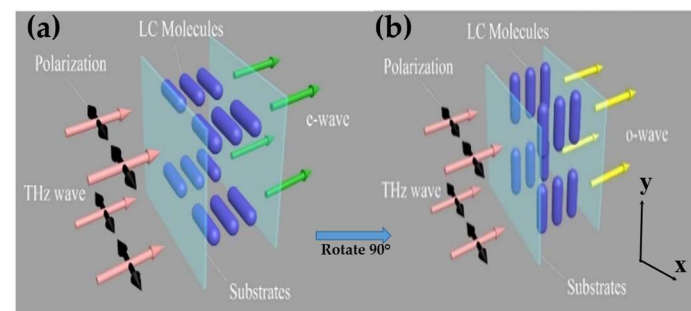
Figure 3. The setup for measuring the birefringence of LC samples: the directors of LC molecules are parallel (**a**) or perpendicular (**b**) to the polarization of the incident THz wave.

3. Results and Discussion

Figure 4a–c show the THz transmission amplitudes of NLC E7, DHFLC 587, and ESH-FLC FD4004N and the empty cell as the reference sample, respectively, in the measurement

range from 0 ps to 30 ps measured by the THz time-domain spectroscopy system. The THz time-domain spectra transmission spectrum of o-wave, e-wave, and empty cells (reference samples) of three LC materials were obtained. It is obvious that there is a certain time delay for each transmission spectrum of these three LC materials with the comparison of the reference samples.

Figure 4. The THz time-domain spectra transmission spectrum of o-wave, e-wave, and empty cells (reference samples) of E7 (**a**), DHFLC (**b**), and FD4004N (**c**).

The information about the refractive indices and extinction coefficient of three different LC materials can be gained by Fourier transform. The transmission spectrums of the experimental sample and reference sample are Fourier transformed as E_{exp} and E_{ref}, respectively. Then, the complex transmission coefficient $H(\omega)$ shows as follows:

$$H(\omega) = \frac{E_{exp}}{E_{ref}} = \rho(\omega)\exp\left[-j\Phi(\omega)\right]. \tag{1}$$

In this equation, ω is the frequency, $\rho(\omega)$ is the magnitude of $H(\omega)$, and $\Phi(\omega)$ is the argument of $H(\omega)$. The refractive index of air in this experiment can be regarded as one. Then, the refractive index $n(\omega)$ and extinction coefficient $k(\omega)$ can be calculated as follows:

$$n(\omega) = \frac{c\Phi(\omega)}{\omega d} + 1, \tag{2}$$

$$k(\omega) = \frac{-c\ln\left\{\rho(\omega)\frac{[n(\omega)+1]^2}{4n(\omega)}\right\}}{\omega d}. \tag{3}$$

In these two equations, c is the light speed in air. d is the gap between two substrates. After these calculations, the refractive index and extinction coefficient of one wave (o-wave or e-wave) for one LC material can be acquired. The results of the other wave (e-wave or o-wave) for the same material can also be obtained by using the experiment and calculation procedures above, but only by rotating the sample by 90°. Finally, the birefringence of

this particular LC material is acquired from the difference in the o-wave and e-wave refractive index.

Figure 5 illustrates the birefringence derived from the refractive index of o-wave and e-wave, and the extinction coefficients of E7, FLC 587, and FLC FD4004N in the THz frequency-domain. The frequency range of the measurements is from 0.2 THz to 1 THz. In Figure 5a,b, the birefringence of NLC E7 remains around 0.14 in this certain frequency range, calculated from the difference between its e-wave index of 1.50 and its o-wave index of 1.36. Both of its o-wave and e-wave extinction coefficient are lower than 0.05, with its extinction coefficient of o-wave (upper green curve) being 0.04 at 1 THz and extinction coefficient of e-wave (upper yellow curve) being 0.014 at 1 THz. Figure 5c,d show the complex refractive indices, birefringence, and extinction coefficients of FLC 587. The birefringence is gradually stabled with the growth of the frequency to 0.115. Its extinction coefficients remain stable at 0.06 for o-wave and 0.04 for e-wave. The same parameters were also tested using FLC FD4004N. In Figure 5e,f, its birefringence remains between around 0.165 and 0.175. This large birefringence of ESHFLC will facilitate the fabrication of the high performance of THz liquid crystal devices, such as the phase shifter. Its e-wave extinction coefficient is around 0.01 smaller than the o-wave extinction coefficient, which ranges from 0.05 to 0.09. The extinction coefficient of extraordinary waves (upper green curve) is smaller than that of ordinary waves (lower yellow curve) since rod-like LCs have more obstacles moving on their short axis than on their long axis. In addition, the extinction coefficient of FLCs is smaller than the result of NLC, showing the low transmission loss of terahertz radiation for the relatively low extinction coefficient.
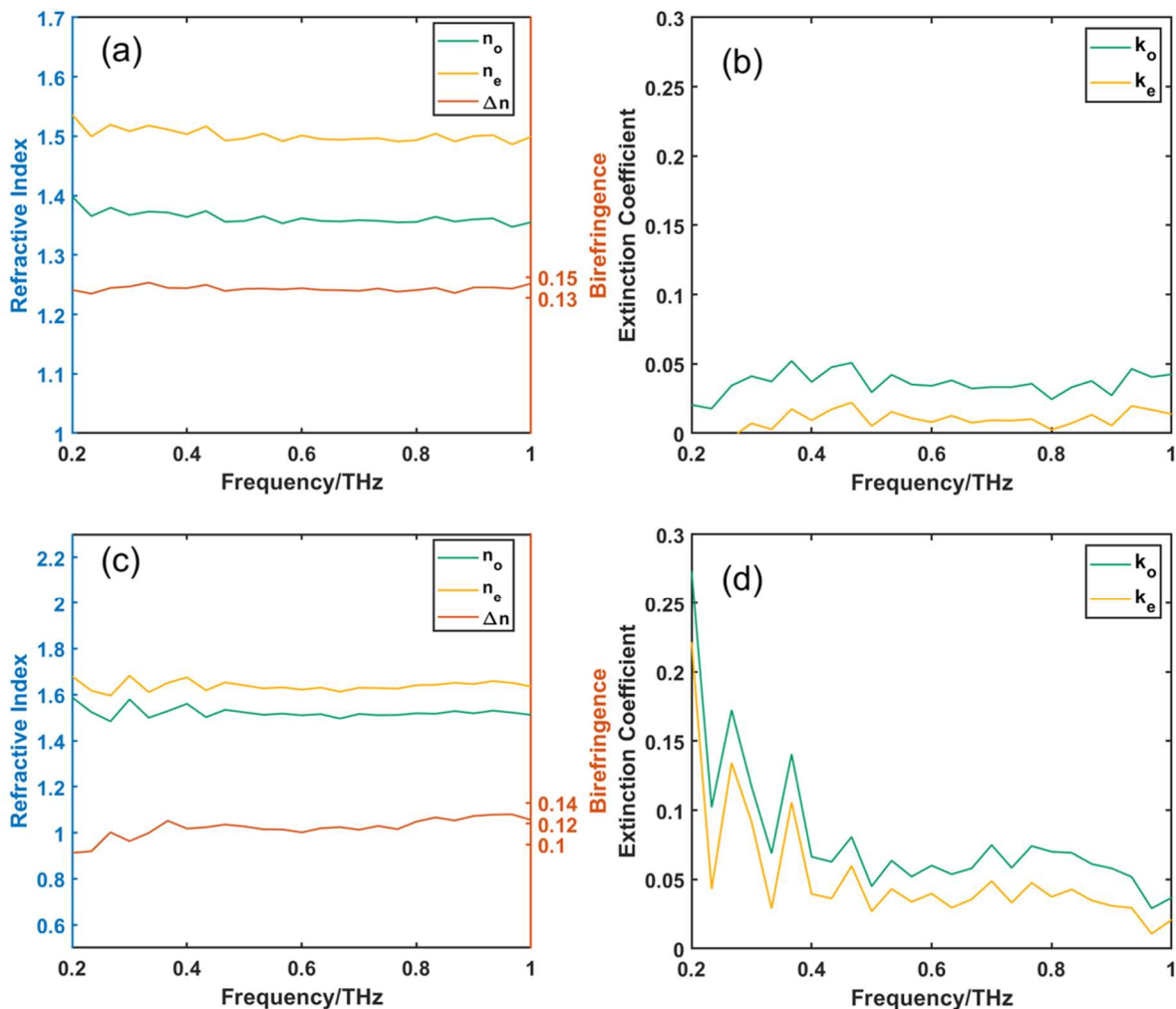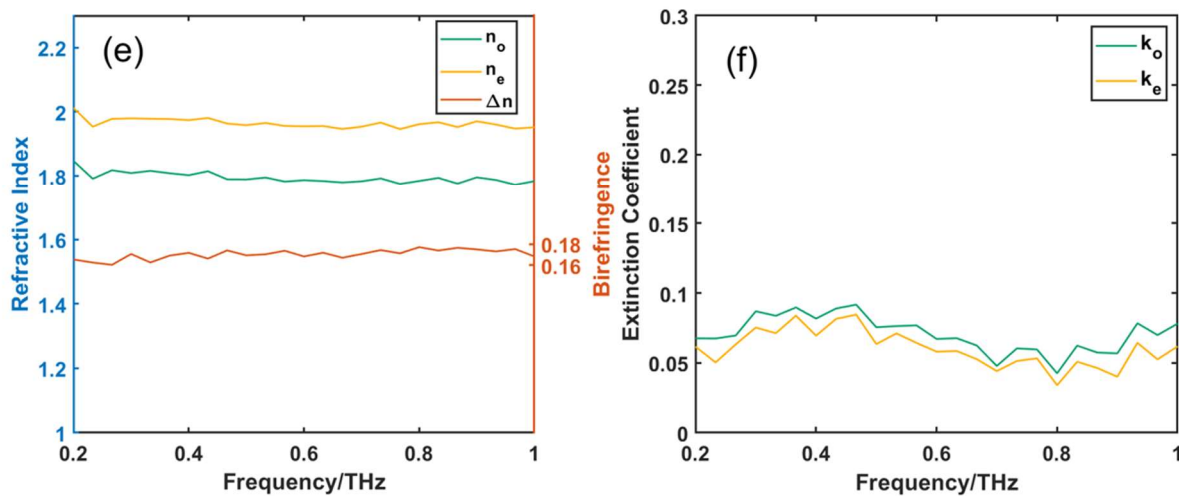

Figure 5. *Cont.*

Figure 5. The complex refractive indices (o-wave refractive index n_o and e-wave refractive index n_e) and birefringence Δn ($\Delta n = n_e - n_o$) of NLC E7 (**a**), FLC 587 (**c**) and FLC FD4004N (**e**) and their corresponding extinction coefficients (o-wave extinction coefficient k_o and e-wave extinction coefficient k_e) (**b**,**d**,**f**) in THz frequency-domain.

4. Conclusions

In conclusion, the refractive index and extinction coefficient of ferroelectric liquid crystal has been examined by the terahertz time-domain spectroscopy system. Two kinds of ferroelectric liquid crystal material, deformed helix ferroelectric liquid crystal and FD4004N, are tested as experimental samples, and E7 nematic liquid crystal is also investigated for comparison. The frequency range of the measurements was from 0.2 THz to 1 THz. The birefringence of DHFLC slowly increases with the growth of frequency, and it averages 0.115, and its extinction coefficient inclines to remain stable at 0.06 for the o-wave extinction coefficient and 0.04 for the e-wave extinction coefficient. The birefringence of FD4004N in the THz frequency-domain remains between around 0.165 and 0.175, and both its e-wave and o-wave extinction coefficients are under 0.1. These results will become useful information for the examination of, adjustment of, and improvement in FLC THz devices. They also provide potential opportunities for fast liquid crystal THz devices.

Institutional Review Board Statement: Not applicable.

Informed Consent Statement: Not applicable.

Data Availability Statement: Data underlying the results presented in this paper are not publicly available at this time but may be obtained from the authors upon reasonable request.

Conflicts of Interest: The authors declare no conflict of interest.

References

1. Pawar, A.Y.; Sonawane, D.D.; Erande, K.B.; Derle, D.V. Terahertz technology and its applications. *Drug Invent. Today* **2013**, *5*, 157–163. [CrossRef]
2. Guerboukha, H.; Nallappan, K.; Skorobogatiy, M. Toward real-time terahertz imaging. *Adv. Opt. Photonics* **2018**, *10*, 843–938. [CrossRef]
3. Chan, W.L.; Deibel, J.; Mittleman, D.M. Imaging with terahertz radiation. *Rep. Prog. Phys.* **2007**, *70*, 1325–1379. [CrossRef]

4. Stantchey, R.L.; Yu, X.; Blu, T.; Pickwell-MacPherson, E. Real-time terahertz imaging with a single-pixel detector. *Nat. Commun.* **2020**, *11*, 8. [CrossRef]
5. Bennett, D.B.; Taylor, Z.D.; Tewari, P.; Singh, R.S.; Culjat, M.O.; Grundfest, W.S.; Sassoon, D.J.; Johnson, R.D.; Hubschman, J.P.; Brown, E.R. Terahertz sensing in corneal tissues. *J. Biomed. Opt.* **2011**, *16*, 8. [CrossRef]
6. Beruete, M.; Jauregui-Lopez, I. Terahertz Sensing Based on Metasurfaces. *Adv. Opt. Mater.* **2020**, *8*, 26. [CrossRef]
7. Singh, R.; Cao, W.; Al-Naib, I.; Cong, L.Q.; Withayachumnankul, W.; Zhang, W.L. Ultrasensitive terahertz sensing with high-Q Fano resonances in metasurfaces. *Appl. Phys. Lett.* **2014**, *105*, 5. [CrossRef]
8. Cao, P.F.; Li, C.C.; Li, Y.; Wu, Y.Y.; Chen, X.Y.; Wu, T.; Zhang, X.Q.; Yuan, M.R.; Wang, Z.L. Electromagnetically Induced Transparency-Like Approach Based on Terahertz Metamaterials for Ultrasensitive Refractive Index Sensors. *IEEE Sens. J.* **2022**, *22*, 2110–2118. [CrossRef]
9. Huang, K.-C.; Wang, Z. Terahertz terabit wireless communication. *IEEE Microw. Mag.* **2011**, *12*, 108–116. [CrossRef]
10. Krumbholz, N.; Gerlach, K.; Rutz, F.; Koch, M.; Piesiewicz, R.; Kürner, T.; Mittleman, D. Omnidirectional terahertz mirrors: A key element for future terahertz communication systems. *Appl. Phys. Lett.* **2006**, *88*, 202905. [CrossRef]
11. Mumtaz, S.; Jornet, J.M.; Aulin, J.; Gerstacker, W.H.; Dong, X.; Ai, B. Terahertz communication for vehicular networks. *IEEE Trans. Veh. Technol.* **2017**, *66*, 5617–5625.
12. Fan, F.; Zhao, H.J.; Ji, Y.Y.; Jiang, S.L.; Tan, Z.Y.; Cheng, J.R.; Chang, S.J. Spin-Decoupled Beam Steering with Active Optical Chirality Based on Terahertz Liquid Crystal Chiral Metadevice. *Adv. Mater. Interfaces* **2023**, *9*, 2202103. [CrossRef]
13. Song, H.-J.; Lee, N. Terahertz Communications: Challenges in the Next Decade. *IEEE Trans. Terahertz Sci. Technol.* **2022**, *12*, 105–117. [CrossRef]
14. Zaytsev, K.; Dolganova, I.; Chernomyrdin, N.; Katyba, G.; Gavdush, A.; Cherkasova, O.; Komandin, G.; Shchedrina, M.; Khodan, A.; Ponomarev, D. The progress and perspectives of terahertz technology for diagnosis of neoplasms: A review. *J. Opt.* **2019**, *22*, 013001. [CrossRef]
15. Brun, M.-A.; Formanek, F.; Yasuda, A.; Sekine, M.; Ando, N.; Eishii, Y. Terahertz imaging applied to cancer diagnosis. *Phys. Med. Biol.* **2010**, *55*, 4615. [CrossRef]
16. Parrott, E.P.J.; Sun, Y.; Pickwell-MacPherson, E. Terahertz spectroscopy: Its future role in medical diagnoses. *J. Mol. Struct.* **2011**, *1006*, 66–76. [CrossRef]
17. Reid, C. *Spectroscopic Methods for Medical Diagnosis at Terahertz Wavelengths*; UCL (University College London): London, UK, 2009.
18. Hermans, R.I.; Seddon, J.; Shams, H.; Ponnampalam, L.; Seeds, A.J.; Aeppli, G. Ultra-high-resolution software-defined photonic terahertz spectroscopy. *Optica* **2020**, *7*, 1445–1455. [CrossRef]
19. Sengupta, K.; Nagatsuma, T.; Mittleman, D.M. Terahertz integrated electronic and hybrid electronic–photonic systems. *Nat. Electron.* **2018**, *1*, 622–635. [CrossRef]
20. Shin, D.C.; Kim, B.S.; Jang, H.; Kim, Y.J.; Kim, S.W. Photonic comb-rooted synthesis of ultra-stable terahertz frequencies. *Nat. Commun.* **2023**, *14*, 10. [CrossRef]
21. Xu, S.T.; Fan, F.; Cao, H.Z.; Wang, Y.H.; Chang, S.J. Liquid crystal integrated metamaterial for multi-band terahertz linear polarization conversion. *Chin. Opt. Lett.* **2021**, *19*, 6. [CrossRef]
22. Degl'Innocenti, R.; Jessop, D.S.; Shah, Y.D.; Sibik, J.; Zeitler, J.A.; Kidambi, P.R.; Hofmann, S.; Beere, H.E.; Ritchie, D.A. Terahertz optical modulator based on metamaterial split-ring resonators and graphene. *Opt. Eng.* **2014**, *53*, 057108. [CrossRef]
23. Liang, G.; Hu, X.; Yu, X.; Shen, Y.; Li, L.H.; Davies, A.G.; Linfield, E.H.; Liang, H.K.; Zhang, Y.; Yu, S.F. Integrated terahertz graphene modulator with 100% modulation depth. *ACS Photonics* **2015**, *2*, 1559–1566. [CrossRef]
24. Yu, H.G.; Wang, H.C.; Shen, Z.X.; Tao, S.N.; Ge, S.J.; Hu, W. Photo-reconfigurable and electrically switchable spatial terahertz wave modulator Invited. *Chin. Opt. Lett.* **2023**, *21*, 5. [CrossRef]
25. Collings, P.J.; Patel, J.S. *Handbook of Liquid Crystal Research*; Swarthmore College: Swarthmore, PA, USA, 1997.
26. Zheng, Z.; Hu, H.; Zhang, Z.; Liu, B.; Li, M.; Qu, D.-H.; Tian, H.; Zhu, W.-H.; Feringa, B.L. Digital photoprogramming of liquid-crystal superstructures featuring intrinsic chiral photoswitches. *Nat. Photonics* **2022**, *16*, 226–234. [CrossRef]
27. Liu, J.; Song, Z.P.; Sun, L.Y.; Li, B.X.; Lu, Y.Q.; Li, Q. Circularly polarized luminescence in chiral orientationally ordered soft matter systems. *Responsive Mater.* **2023**, *1*, e20230005. [CrossRef]
28. Wu, S.-T. Birefringence dispersions of liquid crystals. *Phys. Rev. A* **1986**, *33*, 1270. [CrossRef]
29. Ji, Y.-Y.; Fan, F.; Wang, X.-H.; Chang, S.-J. Broadband controllable terahertz quarter-wave plate based on graphene gratings with liquid crystals. *Opt. Express* **2018**, *26*, 12852–12862. [CrossRef]
30. Hsieh, C.-F.; Yang, C.-S.; Shih, F.-C.; Pan, R.-P.; Pan, C.-L. Liquid-crystal-based magnetically tunable terahertz achromatic quarter-wave plate. *Opt. Express* **2019**, *27*, 9933–9940. [CrossRef]
31. Yang, J.; Xu, L.; Zhang, G.Z.; Li, X.P.; Li, Y.; Hu, M.G.; Li, J.; Lu, H.B.; Deng, G.S.; Yin, Z.P. Rapid terahertz wave manipulation in a liquid-crystal-integrated metasurface structure. *Opt. Express* **2022**, *30*, 33014–33021. [CrossRef] [PubMed]
32. Sahoo, A.K.; Lin, Y.H.; Yang, C.S.; Wada, O.; Yen, C.L.; Pan, C.L. Electrically tunable dual-layer twisted nematic liquid crystal THz phase shifters with intermediate composite polymer thin film. *Opt. Mater. Express* **2022**, *12*, 4733–4754. [CrossRef]
33. Wang, L.; Lin, X.-W.; Hu, W.; Shao, G.-H.; Chen, P.; Liang, L.-J.; Jin, B.-B.; Wu, P.-H.; Qian, H.; Lu, Y.-N.; et al. Broadband tunable liquid crystal terahertz waveplates driven with porous graphene electrodes. *Light Sci. Appl.* **2015**, *4*, e253. [CrossRef]
34. Wang, J.; Tian, H.; Wang, Y.; Li, X.; Cao, Y.; Li, L.; Liu, J.; Zhou, Z. Liquid crystal terahertz modulator with plasmon-induced transparency metamaterial. *Opt. Express* **2018**, *26*, 5769–5776. [CrossRef] [PubMed]

35. Lin, S.; Tang, Y.; Kang, W.; Bisoyi, H.K.; Guo, J.; Li, Q. Photo-triggered full-color circularly polarized luminescence based on photonic capsules for multilevel information encryption. *Nat. Commun.* **2023**, *14*, 3005. [CrossRef] [PubMed]

36. Liu, J.; Song, Z.P.; Wei, J.; Wu, J.J.; Wang, M.Z.; Li, J.G.; Ma, Y.; Li, B.X.; Lu, Y.Q.; Zhao, Q. Circularly Polarized Organic Ultralong Room-Temperature Phosphorescence with A High Dissymmetry Factor in Chiral Helical Superstructures. *Adv. Mater.* **2023**, 2306834. [CrossRef] [PubMed]

37. Cho, S.; Yoshida, H.; Ozaki, M. Tunable polarization volume gratings based on blue phase liquid crystals. *Opt. Express* **2022**, *30*, 1607–1614. [CrossRef] [PubMed]

38. Li, Y.; Yin, Z.; Luo, D. Fabrication and application of free-standing fiber based on blue phase liquid crystal. *Opt. Lett.* **2023**, *48*, 89–92. [CrossRef]

39. Li, Y.; Zhan, T.; Wu, S.-T. Flat cholesteric liquid crystal polymeric lens with low f-number. *Opt. Express* **2020**, *28*, 5875–5882. [CrossRef]

40. Zeng, T.; Xie, J.; Zhou, Y.; Fan, F.; Wen, S. Selectively reflective edge detection system based on cholesteric liquid crystal. *Opt. Lett.* **2023**, *48*, 795–798. [CrossRef]

41. Mukherjee, S.; Yuan, Z.-N.; Sun, Z.-B.; Li, A.-R.; Kang, C.-B.; Kwok, H.-S.; Srivastava, A.K. Fast refocusing lens based on ferroelectric liquid crystals. *Opt. Express* **2021**, *29*, 8258–8267. [CrossRef]

42. Sun, Z.-B.; Yuan, Z.-N.; Nikita, A.; Kwok, H.-S.; Srivastava, A.K. Fast-switchable, high diffraction-efficiency ferroelectric liquid crystal Fibonacci grating. *Opt. Express* **2021**, *29*, 13978–13986. [CrossRef]

43. Liu, Q.F.; Luo, D.; Li, S.X.; Tian, Z. The birefringence and extinction coefficient of positive and negative liquid crystals in the terahertz range. *Liq. Cryst.* **2016**, *43*, 796–802. [CrossRef]

44. Liu, Q.; Luo, D.; Zhang, X.; Li, S.; Tian, Z. Refractive index and absorption coefficient of blue phase liquid crystal in terahertz band. *Liq. Cryst.* **2017**, *44*, 348–354. [CrossRef]

45. Pozhidaev, E.P.; Kiselev, A.D.; Srivastava, A.K.; Chigrinov, V.G.; Kwok, H.-S.; Minchenko, M.V. Orientational Kerr effect and phase modulation of light in deformed-helix ferroelectric liquid crystals with subwavelength pitch. *Phys. Rev. E* **2013**, *87*, 052502. [CrossRef] [PubMed]